

Measurement-Induced Phase Transition in Free Bosons

Kazuki Yokomizo¹ and Yuto Ashida^{1,2}

¹*Department of Physics, The University of Tokyo,
7-3-1 Hongo, Bunkyo-ku, Tokyo, 113-0033, Japan*

²*Institute for Physics of Intelligence, University of Tokyo, 7-3-1 Hongo, Tokyo 113-0033, Japan*

The competition between quantum many-particle dynamics and continuous monitoring can lead to measurement-induced phase transitions (MIPTs). So far, MIPTs have been much explored in fermionic or spin systems. To examine the possibility of a MIPT in bosonic systems, we study the entanglement structure in continuously monitored free bosons with long-range couplings. When the measurement is local, we find that no MIPTs occur because the substantial entanglement generated by the long-range coupling overcome the entanglement destruction due to the measurement. In contrast, we show that the nonlocal measurement can efficiently suppress the entanglement generation, leading to a MIPT where the bipartite entanglement entropy exhibits the subvolume-to-area law transition as the measurement strength is increased. Possible experimental relevance to levitated nanoparticle arrays is also briefly discussed.

Quantum entanglement lies at the heart of quantum physics and quantum technologies [1, 2]. While unitary dynamics can generate entanglement, nonunitary time evolution induced by quantum measurements tends to destroy entanglement. The competition between the generation and destruction of entanglement can give rise to a phase transition at the level of single quantum trajectory, where the dynamics is conditioned on measurement outcomes. Such a measurement-induced phase transition (MIPT) manifests itself as the transition in the size scaling of the bipartite entanglement entropy.

Previous theoretical studies on quantum circuits have demonstrated that the increase in the rate of random projection measurements can lead to the transition of the entanglement scaling from the volume law to the area law [3–19], and some of the predictions have been tested experimentally [20–22]. MIPTs have been also explored in quantum many-body systems under continuous quantum measurements, where the entanglement entropy of quantum trajectories has been found to exhibit a volume-to-area law transition as the measurement strength is increased [23–29].

Nevertheless, the fate of MIPTs in free-particle systems is still under debate. In one-dimensional (1D) free fermions with short-range couplings, an early study [30] and recent field-theoretical analysis [31, 32] have proposed the area law at any nonzero measurement strength, while the signatures of possible critical logarithmic-law phases have been observed in several studies [33, 34]. Meanwhile, in 1D free fermions with long-range couplings, the presence of the subvolume-to-area law transition has been predicted [35, 36]. So far, however, previous studies have focused on fermionic or spin systems in which the dimension of the Hilbert space is finite. The situation in bosonic systems, where even a local Hilbert space is unbounded, has been much less explored. It is thus timely to ask under what conditions a bosonic MIPT can occur.

In this Letter, we investigate the entanglement struc-

ture in typical individual quantum trajectories of free bosons under continuous monitoring. Specifically, we consider an array of particles [Fig. 1(a)], each of which is trapped in a harmonic potential. The particles interact with each other via the long-range coupling obeying the power-law decay $r^{-\alpha}$ with the distance r between the particles. The particle positions are continuously monitored via a Gaussian measurement, where a quantum state can be described by a pure bosonic Gaussian state during

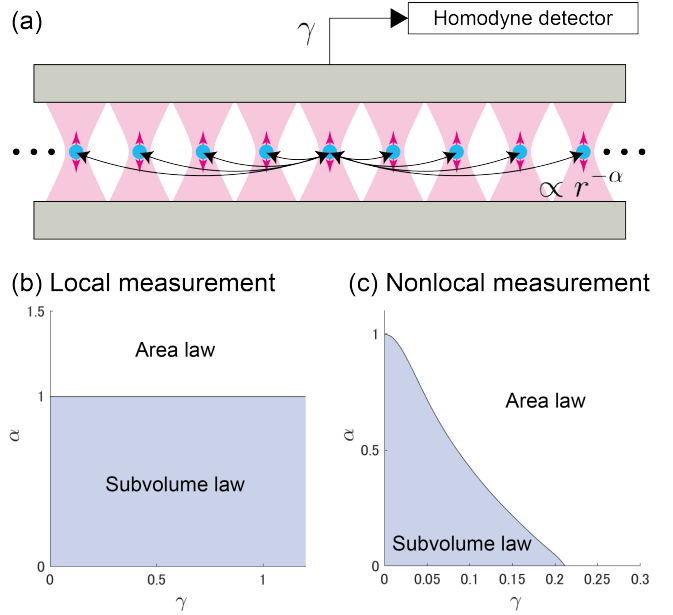


FIG. 1. (a) Schematic illustration of the setup. The red arrows represent the direction of the particle motion. The particles interact with each other via the long-range coupling whose strength is proportional to $r^{-\alpha}$ with the distance r . We denote the measurement strength by γ and set the number of the particles to be L . (b,c) Phase diagrams of the half-chain entanglement entropy S under the (b) local or (c) nonlocal measurement, where the subvolume-law phase (area-law phase) exhibits the scaling $S \propto L^b$ with $0 < b < 1$ ($S \propto L^0$).

the time evolution; this fact allows us to efficiently calculate the bipartite entanglement entropy S in the long-time limit for a relatively large systems size L . Remarkably, we find two distinct types of the phase diagrams [Figs. 1(b) and (c)] depending on whether measurement is short- or long-ranged. Both phase diagrams include the subvolume-law phase with $S \propto L^b$ ($0 < b < 1$) and the are-law phase with $S \propto L^0$. The main difference between the two cases is that the MIPT, a transition occurring as a function of the measurement strength γ , can appear only in the case of the nonlocal measurement [Fig. 1(c)]. The absence of the MIPT under the local measurement [Fig. 1(b)] is reminiscent of the previous finding in free fermions [36]. When taking the short-range limit $\alpha \rightarrow \infty$ in the present setup, our analysis reproduces a recent result [37] where the area law with no phase transitions has been found. Altogether, our results indicate that the long-rangedness in both particle couplings and measurements is crucial for the MIPT to occur in free-bosonic systems.

Before getting into details, we mention that our study is partly motivated by recent advances in the control of levitated nanoparticles [38, 39]. Indeed, it has been experimentally demonstrated that multiple levitated nanoparticles can be prepared in a tunable manner, and they exhibit the long-range interaction with the power-law decay [40]. Furthermore, it has been proposed that continuous observation of the dynamics of trapped particles can be realized by measuring the scattered light via homodyne detection [41]. Our results thus show that nontrivial measurement-induced phenomena can occur in such continuous-variable quantum systems under quantum measurements.

To be concrete, we consider the array consisting of L particles that are placed periodically and subject to an open boundary condition. The dynamics of the particles is described by a set of the position and momentum operators denoted by $\hat{\phi} = (\hat{x}_1, \dots, \hat{x}_L, \hat{p}_1, \dots, \hat{p}_L)^T$, which satisfy the commutation relations

$$[\hat{\phi}_j, \hat{\phi}_k] = i\sigma_{jk}, \quad \sigma = \begin{pmatrix} O & 1_L \\ -1_L & O \end{pmatrix}, \quad (1)$$

where 1_L is an $L \times L$ identity matrix, and we set $\hbar = 1$. The total Hamiltonian reads

$$\hat{H} = \sum_{j=1}^L \frac{\Omega}{2} (\hat{p}_j^2 + \hat{x}_j^2) + \sum_{j=1}^{L-1} \sum_{r=1}^{L-j} \frac{K}{2r^\alpha} (\hat{x}_j - \hat{x}_{j+r})^2, \quad (2)$$

where Ω and K are the trap frequency and the coupling strength, respectively, and α is the exponent that characterizes the power-law decay of the long-range coupling. We note that the short-range coupling corresponds to taking the limit $\alpha \rightarrow \infty$. For the sake of simplicity, we assume $\Omega = K = 1$ throughout this Letter.

The particles are subject to a continuous Gaussian measurement described by a Hermitian jump operator

$\hat{\mathcal{O}}_n$, which is given by a linear combination of $\hat{\phi}_j$. We emphasize that the support of $\hat{\mathcal{O}}_n$ is not necessarily restricted to a local region; for instance, we will later consider the case of the nonlocal measurement where $\hat{\mathcal{O}}_n$ acts on the distant particles. In the diffusive limit [42–46], the time evolution of a quantum many-body state $|\psi\rangle$ is governed by the stochastic Schrödinger equation,

$$d|\psi\rangle = \left[-i\hat{H}dt - \frac{1}{2} \sum_n (\hat{\mathcal{O}}_n - \langle \hat{\mathcal{O}}_n \rangle)^2 dt + \sum_n (\hat{\mathcal{O}}_n - \langle \hat{\mathcal{O}}_n \rangle) dW_n \right] |\psi\rangle, \quad (3)$$

where dW_n is the Wiener increment satisfying $\mathbb{E}[dW_n] = 0$ and $dW_n dW_m = \delta_{nm} dt$. Here, $\mathbb{E}[\dots]$ represents the ensemble average over the measurement outcomes, and $\langle \dots \rangle$ is the expectation value with respect to $|\psi\rangle$. Suppose that the initial state is a bosonic Gaussian state, whose Wigner function can be written as the Gaussian form [47]. Since we consider a quadratic Hamiltonian and a Gaussian measurement, a quantum state remains to be Gaussian during the whole time evolution. Here, it is worthwhile to recall that a bosonic Gaussian state $|\psi_G\rangle$ can be fully characterized by its mean value $\langle \phi \rangle = \langle \psi_G | \hat{\phi} | \psi_G \rangle$ and covariance matrix,

$$(\Gamma_\phi)_{jk} = \frac{1}{2} \langle \psi_G | \{\delta\hat{\phi}_j, \delta\hat{\phi}_k\} | \psi_G \rangle \quad (4)$$

with $j, k = 1, \dots, 2L$ and $\delta\hat{\phi}_j = \hat{\phi}_j - \langle \psi_G | \hat{\phi}_j | \psi_G \rangle$.

A key quantity to analyze the entanglement structure of the typical quantum trajectory is the ensemble-averaged entanglement entropy in the steady-state regime. Specifically, we divide the whole system into two regions A and \bar{A} and introduce the reduced density operator $\hat{\rho}_A = \text{Tr}_{\bar{A}}[|\psi\rangle \langle \psi|]$ for each quantum trajectory. We then define the typical entanglement entropy S_A by taking the ensemble average of the von Neumann entropy over the measurement outcomes:

$$S_A = -\mathbb{E}[\text{Tr}(\hat{\rho}_A \log \hat{\rho}_A)]. \quad (5)$$

Importantly, the analysis of S_A can be greatly simplified in the present setup because the time evolution of the covariance matrix turns out to be deterministic and has a unique steady solution. Said differently, the covariance matrix of each quantum trajectory always converges to the same steady-state value in the long-time limit [37]. Consequently, the ensemble average in Eq. (5) is not necessary, but it suffices to analyze the covariance matrix in the steady-state regime.

Below, we focus on the half-chain entanglement en-

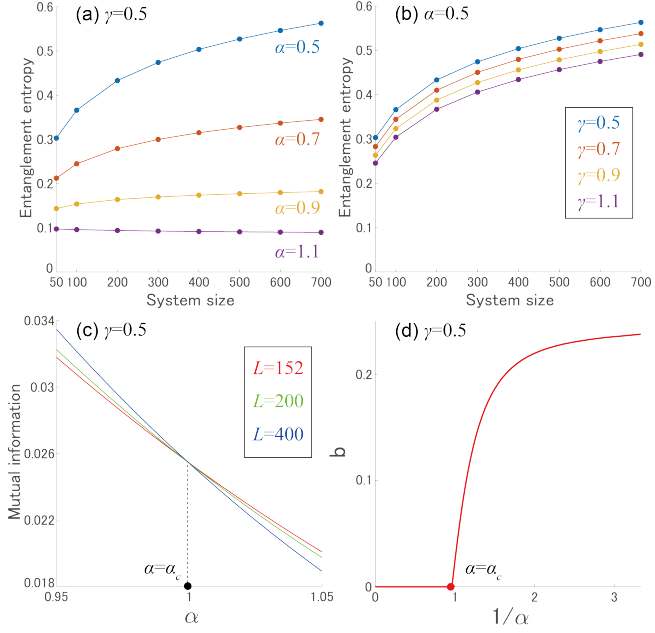


FIG. 2. Entanglement entropy and mutual information under the local measurement. (a,b) Half-chain entanglement entropy S_A . The parameters are $\gamma = 0.5$ with varying α in (a) and $\alpha = 0.5$ with varying γ in (b). (c) Mutual information I_{BC} at $\gamma = 0.5$. The entanglement phase transition occurs at $\alpha_c = 1$. (d) Size-scaling exponent b extracted from the fitting to $S_A = aL^b$.

tropy with $A = \{j | 1 \leq j \leq L/2\}$ given by

$$S_A = \sum_{l=1}^{L/2} \left[\left(\kappa_l + \frac{1}{2} \right) \log \left(\kappa_l + \frac{1}{2} \right) - \left(\kappa_l - \frac{1}{2} \right) \log \left(\kappa_l - \frac{1}{2} \right) \right], \quad (6)$$

where κ_l ($l = 1, \dots, L/2$) are the symplectic eigenvalues of the submatrix of the covariance matrix (4) corresponding to the subregion A [48]. We also analyze the mutual information $I_{BC} = S_B + S_C - S_{B \cup C}$ between distant subregions B and C , which can be used as yet another indicator of a MIPT. To be concrete, we choose the subregions B and C to be $\{j | L/4 + 1 \leq j \leq 3L/8\}$ and $\{j | 5L/8 + 1 \leq j \leq 3L/4\}$, respectively.

We first consider the case of the local measurement defined by the jump operator,

$$\hat{O}_n = \sqrt{\gamma} \hat{x}_n, \quad (n = 1, \dots, L), \quad (7)$$

which acts on each particle and includes the parameter $\gamma (> 0)$ as the measurement strength. In this case, on the one hand, it has been known that no MIPTs are expected in the short-range limit $\alpha \rightarrow \infty$ because the correlation function decays exponentially and the entanglement entropy obeys the area law at any measurement strength [37]. On the other hand, however, the long-range coupling with a finite α can efficiently transfer

the quantum information between the distant particles and should facilitate the entanglement generation. As α is decreased, the enhanced entanglement generation is expected to eventually overcome the entanglement destruction due to the measurement. Indeed, as shown in Fig. 2(a), we find that the entanglement scaling changes from the area law to the subvolume law at a threshold value α_c . Accordingly, the correlation function exhibits the exponential decay when $\alpha > \alpha_c$, while it almost does not decay even at large distances when $\alpha < \alpha_c$ [48].

To accurately locate the critical point, we investigate the dependence of the mutual information on α at different system sizes [Fig. 2(c)]. The numerical data intersecting at the same point indicates the transition at $\alpha_c = 1$, and we find that this value is independent of the measurement strength. The resulting phase diagram is shown in Fig. 1(b).

Physically, these findings can be understood from the similar argument as in the case of free fermions [35]. Namely, the growth rate of the entanglement entropy, which is characterized by the operator norm of the interaction Hamiltonian between subregions A and \bar{A} , is expected to diverge in the thermodynamic limit at $\alpha < 1$, and the local measurement is simply not enough to suppress such substantial entanglement growth.

In the subvolume phase at $\alpha < \alpha_c$, the entanglement entropy obeys the algebraic scaling, $S_A \propto L^b$ with $0 < b < 1$. Figure 2(d) shows the dependence of the size-scaling exponent b on $1/\alpha$, which again confirms the transition at $\alpha_c = 1$. Interestingly, we find that changing the measurement strength has no effects on the size-scaling exponent of the entanglement entropy [cf. Fig. 2(b)]. All in all, under the local measurement, the system can exhibit the entanglement transition which essentially originates from the diverging growth rate of the entanglement generated by the long-range coupling rather than the nontrivial competition with the measurement. In this respect, we argue that the free bosons under the local measurement do not show a MIPT that should occur as a function of the measurement strength.

To explore the possibility of MIPTs in bosonic systems, we next consider the system under the nonlocal measurement represented by

$$\hat{O}_n = \sqrt{\frac{\gamma}{r^\alpha}} (\hat{x}_j \pm \hat{x}_{j+r}). \quad (8)$$

Here, $n = (j, r, \pm)$ now includes a set of the indices, where j and r define the particle positions that the jump operator acts on, and \pm characterizes whether the jump operator is symmetric or antisymmetric combination of the position operators. The nonlocality here refers to the fact that the jump operator acts on the two distant particles. We note that this choice of the measurement operator is naturally motivated from recent studies in levitated nanoparticles as discussed later.

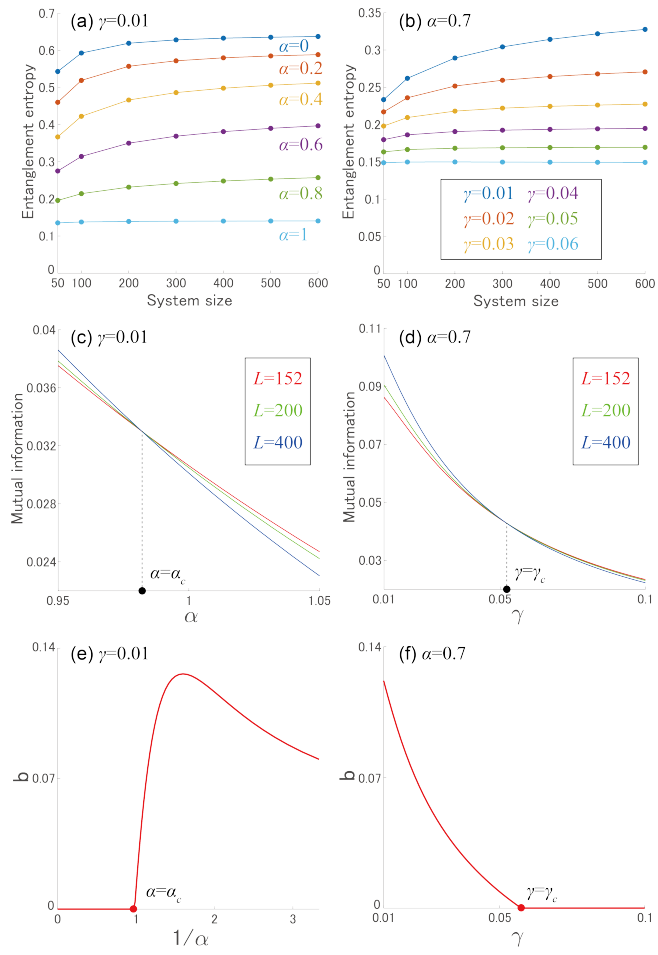


FIG. 3. Entanglement entropy and mutual information under the nonlocal measurement. (a,b) Half-chain entanglement entropy S_A . (c,d) Mutual information I_{BC} plotted against α in (c) and γ in (d). (e,f) Size-scaling exponent b extracted from the fitting to $S_A = aL^b$. The parameters are $\gamma = 0.01$ in (a,c,e) and $\alpha = 0.7$ in (b,d,f).

Because of the nonlocal nature of the jump operator, we expect that the measurement can now suppress the rapid entanglement growth generated by the long-range coupling more efficiently. Indeed, we find that the system undergoes the subvolume-to-area law transition as either the measurement strength γ or the exponent α is increased [Figs. 3(a) and (b)], making a sharp contrast to the case of the local measurement. Accordingly, the phase boundary now depends on γ in addition to α as shown in Fig. 1(c), where we numerically determine the transition point by locating the intersecting point in the mutual information [see, e.g., Figs. 3(c) and (d)]. The key feature is that, when $\alpha < 1$, there occurs the MIPT as the measurement strength exceeds the threshold value γ_c .

In the subvolume law phase at $\gamma < \gamma_c$, the half-chain entanglement entropy obeys $S_A \propto L^b$ with $0 < b < 1$, similar to the case of the local measurement. Figures 3(e)

and (f) plot the size-scaling exponent b as a function of $1/\alpha$ and γ , respectively. The critical points in both Figs. 3(e) and (f) agree with the ones extracted from the mutual information in Figs. 3(c) and (d). This agreement provides a further evidence of the presence of the MIPT in the free-bosonic systems. We note that, in Fig. 3(e), there is an optimal α at which the size-scaling exponent becomes maximal. This nonmonotonic behavior is absent in the case of the local measurement [cf. Fig. 2(d)] and should have its roots in the fact that the nonlocal measurement tends to overcome the entanglement generation in the infinite-range limit $1/\alpha \rightarrow \infty$ [48].

Finally, we briefly discuss the case of the short-ranged free bosons under the nonlocal measurement described by Eq. (8) [49]; a similar setup has recently been considered in Ref. [29] for free fermions. Our result shows no evidences of entanglement transitions, where the entanglement entropy always obeys the area law [48]. We thus conclude that the long-range coupling is crucial to stabilize the subvolume-law phase in free bosons under continuous monitoring.

We briefly discuss possible experimental relevance of our setup illustrated in Fig. 1(a). The array of continuous-variable quantum systems considered here would be prepared by periodically arranging multiple levitated nanoparticles, which are subwavelength microscopic objects optically trapped by lasers [38, 39]. A single levitated nanoparticle oscillates along the optical axis in the vicinity of the focal plane, and its center-of-mass motion can be modeled as a harmonic oscillator. Arranging the two levitated nanoparticles, the interference occurs between the scattered light from the particle and the trapping laser, and the two particles are coupled by the long-range interaction known as the optical binding force [40]. Measuring the light scattered from the particles by, e.g., homodyne detection, one might implement the continuous monitoring of the particle positions [41]. Extending this to a multiparticle setup considered here, the stochastic quantum dynamics of the monitored levitated nanoparticles can be described by Eq. (3) in the ideal limit of the perfect detection efficiency. For instance, the local jump operator in Eq. (7) corresponds to the position measurement of each particle, while the nonlocal one in Eq. (8) could be realized by conducting the basis transformation in the homodyne detection of the two distant particles [41].

In summary, we examine under what conditions the MIPT can occur in the free-bosonic systems under continuous monitoring. Our key finding is that the MIPT, a transition induced by increasing the measurement strength, can occur only when both particle-particle couplings and measurements are long-ranged. We confirm this by evaluating the half-chain entanglement entropy and the mutual information of the bosonic Gaussian state obeying the stochastic Schrödinger equation. The results are summarized in the phase diagrams in Figs. 1(b) and

(c); under the local measurement, the phase boundary between the subvolume-law and area-law phases is insensitive to the measurement strength γ , while the boundary acquires the γ dependence in the case of the nonlocal measurement, thus leading to the MIPT. We also briefly discuss the possible experimental relevance of our setup to levitated nanoparticle arrays.

Several interesting directions remain for future studies. First, it would be intriguing to ask how one can construct an effective field theory of free bosons under nonlocal measurements. In particular, it merits further study to identify the universality class of the MIPT found in the present work. The fate of MIPTs in higher-dimensional bosonic systems also remains an interesting open problem.

Second, we note that the Lindblad evolution of the present setup, which corresponds to the dynamics obtained after taking the ensemble average, correctly reproduces the equations of motion for the dissipative dynamics of levitated nanoparticle arrays that have been originally considered in the classical regime [50]. There, one can implement the nonreciprocal dipole-dipole interaction as experimentally realized in the case of two levitated nanoparticles [40]. It would be interesting to explore the role of nonreciprocal interaction in a full-fledged quantum trajectory in monitored many-particle systems beyond no-click limit [51, 52].

Finally, it is also natural to investigate the entanglement structure in the ensemble-averaged density operator rather than the one in the typical quantum trajectory considered here. Our initial analysis shows that the half-chain logarithmic negativity vanishes in short time [48]. While the vanishment of the logarithmic negativity does not imply the separability in general, necessary and sufficient criteria for the separability of a bosonic Gaussian state has been known [53, 54]. It merits further study to understand the entanglement structure of levitated nanoparticle arrays under decoherence from the viewpoint of those criteria.

We are grateful to Yohei Fuji, Keisuke Fujii, Zongping Gong, Keiji Saito, and Benjamin A. Stickler for variable discussion. K.Y. is supported by JSPS KAKENHI through Grant No. JP21J01409. Y.A. acknowledges support from the Japan Society for the Promotion of Science through Grant No. JP19K23424 and from JST FOREST Program (Grant No. JPMJFR222U, Japan).

ment, *Phys. Rev. X* **9**, 031009 (2019).

- [4] Y. Li, X. Chen, and M. P. A. Fisher, *Measurement-driven entanglement transition in hybrid quantum circuits*, *Phys. Rev. B* **100**, 134306 (2019).
- [5] Q. Tang and W. Zhu, *Measurement-induced phase transition: A case study in the nonintegrable model by density-matrix renormalization group calculations*, *Phys. Rev. Res.* **2**, 013022 (2020).
- [6] A. Zabalo, M. J. Gullans, J. H. Wilson, S. Gopalakrishnan, D. A. Huse, and J. H. Pixley, *Critical properties of the measurement-induced transition in random quantum circuits*, *Phys. Rev. B* **101**, 060301(R) (2020).
- [7] Y. Bao, S. Choi, and E. Altman, *Theory of the phase transition in random unitary circuits with measurements*, *Phys. Rev. B* **101**, 104301 (2020).
- [8] C.-M. Jian, Y.-Z. You, R. Vasseur, and A. W. W. Ludwig, *Measurement-induced criticality in random quantum circuits*, *Phys. Rev. B* **101**, 104302 (2020).
- [9] S. Choi, Y. Bao, X.-L. Qi, and E. Altman, *Quantum Error Correction in Scrambling Dynamics and Measurement-Induced Phase Transition*, *Phys. Rev. Lett.* **125**, 030505 (2020).
- [10] X. Turkeshi, R. Fazio, and M. Dalmonte, *Measurement-induced criticality in (2+1)-dimensional hybrid quantum circuits*, *Phys. Rev. B* **102**, 014315 (2020).
- [11] M. J. Gullans and D. A. Huse, *Scalable Probes of Measurement-Induced Criticality*, *Phys. Rev. Lett.* **125**, 070606 (2020).
- [12] N. Lang and H. P. Büchler, *Entanglement transition in the projective transverse field Ising model*, *Phys. Rev. B* **102**, 094204 (2020).
- [13] M. J. Gullans and D. A. Huse, *Dynamical Purification Phase Transition Induced by Quantum Measurements*, *Phys. Rev. X* **10**, 041020 (2020).
- [14] A. Lavasani, Y. Alavirad, and M. Barkeshli, *Measurement-induced topological entanglement transitions in symmetric random quantum circuits*, *Nat. Phys.* **17**, 342–347 (2021).
- [15] A. Nahum, S. Roy, B. Skinner, and J. Ruhman, *Measurement and Entanglement Phase Transitions in All-To-All Quantum Circuits, on Quantum Trees, and in Landau-Ginsburg Theory*, *PRX Quantum* **2**, 010352 (2021).
- [16] M. Block, Y. Bao, S. Choi, E. Altman, and N. Y. Yao, *Measurement-Induced Transition in Long-Range Interacting Quantum Circuits*, *Phys. Rev. Lett.* **128**, 010604 (2022).
- [17] S. Sharma, X. Turkeshi, R. Fazio, and M. Dalmonte, *Measurement-induced criticality in extended and long-range unitary circuits*, *SciPost Phys. Core* **5**, 023 (2022).
- [18] M. P. Fisher, V. Khemani, A. Nahum, and S. Vijay, *Random quantum circuits*, *Annu. Rev. Condens. Matter Phys.* **14**, 335–379 (2023).
- [19] E. Granet, C. Zhang, and H. Dreyer, *Volume-Law to Area-Law Entanglement Transition in a Nonunitary Periodic Gaussian Circuit*, *Phys. Rev. Lett.* **130**, 230401 (2023).
- [20] C. Noel, P. Niroula, D. Zhu, A. Risinger, L. Egan, D. Biswas, M. Cetina, A. V. Gorshkov, M. J. Gullans, D. A. Huse, and C. Monroe, *Measurement-induced quantum phases realized in a trapped-ion quantum computer*, *Nat. Phys.* **18**, 760–764 (2022).
- [21] J. M. Koh, S.-N. Sun, M. Motta, and A. J. Minnich, *Measurement-induced entanglement phase transition on a superconducting quantum processor with mid-circuit read-*

- [1] R. Horodecki, P. Horodecki, M. Horodecki, and K. Horodecki, *Quantum entanglement*, *Rev. Mod. Phys.* **81**, 865–942 (2009).
- [2] E. Chitambar and G. Gour, *Quantum resource theories*, *Rev. Mod. Phys.* **91**, 025001 (2019).
- [3] B. Skinner, J. Ruhman, and A. Nahum, *Measurement-Induced Phase Transitions in the Dynamics of Entangle-*

out, *Nat. Phys.* **19**, 1314–1319 (2023).

[22] J. C. Hoke *et al.*, (Google Quantum AI and Collaborators), *Measurement-induced entanglement and teleportation on a noisy quantum processor*, *Nature* **622**, 481–486 (2023).

[23] Y. Fuji and Y. Ashida, *Measurement-induced quantum criticality under continuous monitoring*, *Phys. Rev. B* **102**, 054302 (2020).

[24] S. Goto and I. Danshita, *Measurement-induced transitions of the entanglement scaling law in ultracold gases with controllable dissipation*, *Phys. Rev. A* **102**, 033316 (2020).

[25] S. Gopalakrishnan and M. J. Gullans, *Entanglement and Purification Transitions in Non-Hermitian Quantum Mechanics*, *Phys. Rev. Lett.* **126**, 170503 (2021).

[26] X. Turkeshi, A. Biella, R. Fazio, M. Dalmonte, and M. Schirò, *Measurement-induced entanglement transitions in the quantum Ising chain: From infinite to zero clicks*, *Phys. Rev. B* **103**, 224210 (2021).

[27] X. Turkeshi, M. Dalmonte, R. Fazio, and M. Schirò, *Entanglement transitions from stochastic resetting of non-Hermitian quasiparticles*, *Phys. Rev. B* **105**, L241114 (2022).

[28] C. Zerba and A. Silva, *Measurement phase transitions in the no-click limit as quantum phase transitions of a non-hermitean vacuum*, *SciPost Phys. Core* **6**, 051 (2023).

[29] A. Russomanno, G. Piccitto, and D. Rossini, *Entanglement transitions and quantum bifurcations under continuous long-range monitoring*, *Phys. Rev. B* **108**, 104313 (2023).

[30] X. Cao, A. Tilloy, and A. De Luca, *Entanglement in a fermion chain under continuous monitoring*, *SciPost Phys.* **7**, 024 (2019).

[31] I. Pohoiko, P. Pöpperl, I. V. Gornyi, and A. D. Mirlin, *Theory of Free Fermions under Random Projective Measurements*, *Phys. Rev. X* **13**, 041046 (2023).

[32] T. Jin and D. G. Martin, *Measurement-induced phase transition in a single-body tight-binding model*, arXiv:2309.15034 10.48550/arXiv.2309.15034.

[33] O. Alberton, M. Buchhold, and S. Diehl, *Entanglement Transition in a Monitored Free-Fermion Chain: From Extended Criticality to Area Law*, *Phys. Rev. Lett.* **126**, 170602 (2021).

[34] M. Buchhold, Y. Minoguchi, A. Altland, and S. Diehl, *Effective Theory for the Measurement-Induced Phase Transition of Dirac Fermions*, *Phys. Rev. X* **11**, 041004 (2021).

[35] T. Minato, K. Sugimoto, T. Kuwahara, and K. Saito, *Fate of Measurement-Induced Phase Transition in Long-Range Interactions*, *Phys. Rev. Lett.* **128**, 010603 (2022).

[36] T. Müller, S. Diehl, and M. Buchhold, *Measurement-Induced Dark State Phase Transitions in Long-Ranged Fermion Systems*, *Phys. Rev. Lett.* **128**, 010605 (2022).

[37] Y. Minoguchi, P. Rabl, and M. Buchhold, *Continuous gaussian measurements of the free boson CFT: A model for exactly solvable and detectable measurement-induced dynamics*, *SciPost Phys.* **12**, 009 (2022).

[38] C. Gonzalez-Ballester, M. Aspelmeyer, L. Novotny, R. Quidant, and O. Romero-Isart, *Levitodynamics: Levitation and control of microscopic objects in vacuum*, *Science* **374**, eabg3027 (2021).

[39] J. Millen, T. S. Monteiro, R. Pettit, and A. N. Vamivakas, *Optomechanics with levitated particles*, *Rep. Prog. Phys.* **83**, 026401 (2020).

[40] J. Rieser, M. A. Ciampini, H. Rudolph, N. Kiesel, K. Hornberger, B. A. Stickler, M. Aspelmeyer, and U. Delić, *Tunable light-induced dipole-dipole interaction between optically levitated nanoparticles*, *Science* **377**, 987–990 (2022).

[41] H. Rudolph, U. c. v. Delić, M. Aspelmeyer, K. Hornberger, and B. A. Stickler, *Force-Gradient Sensing and Entanglement via Feedback Cooling of Interacting Nanoparticles*, *Phys. Rev. Lett.* **129**, 193602 (2022).

[42] N. Gisin, *Quantum Measurements and Stochastic Processes*, *Phys. Rev. Lett.* **52**, 1657–1660 (1984).

[43] L. Diósi, *Continuous quantum measurement and Itô formalism*, *Phys. Lett. A* **129**, 419–423 (1988).

[44] L. Diósi, *Quantum stochastic processes as models for state vector reduction*, *J. Phys. A: Math. Gen.* **21**, 2885 (1988).

[45] K. Jacobs and D. A. Steck, *A straightforward introduction to continuous quantum measurement*, *Contemp. Phys.* **47**, 279–303 (2006).

[46] Y. Ashida, Z. Gong, and M. Ueda, *Non-hermitian physics*, *Adv. Phys.* **69**, 249–435 (2020).

[47] C. Weedbrook, S. Pirandola, R. García-Patrón, N. J. Cerf, T. C. Ralph, J. H. Shapiro, and S. Lloyd, *Gaussian quantum information*, *Rev. Mod. Phys.* **84**, 621–669 (2012).

[48] See Supplemental Material for descriptions of the bosonic Gaussian state, derivation of the time-evolution equations of the first and second moments, and further discussions about the spatial correlation, entanglement scaling, and logarithmic negativity, which includes Refs. [55–59].

[49] We note that the exponent α here only refers to the long-distance decay in the jump operator in Eq. (7).

[50] K. Yokomizo and Y. Ashida, *Non-Hermitian physics of levitated nanoparticle array*, *Phys. Rev. Res.* **5**, 033217 (2023).

[51] K. Kawabata, T. Numasawa, and S. Ryu, *Entanglement Phase Transition Induced by the Non-Hermitian Skin Effect*, *Phys. Rev. X* **13**, 021007 (2023).

[52] G. Lee, T. Jin, Y.-X. Wang, A. McDonald, and A. Clerk, *Entanglement Phase Transition Due to Reciprocity Breaking without Measurement or Postselection*, *PRX Quantum* **5**, 010313 (2024).

[53] R. F. Werner and M. M. Wolf, *Bound Entangled Gaussian States*, *Phys. Rev. Lett.* **86**, 3658–3661 (2001).

[54] L. Lami, A. Serafini, and G. Adesso, *Gaussian entanglement revisited*, *New J. Phys.* **20**, 023030 (2018).

[55] L. Hackl and E. Bianchi, *Bosonic and fermionic Gaussian states from Kähler structures*, *SciPost Phys. Core* **4**, 025 (2021).

[56] V. I. Arnold, *Mathematical Methods of Classical Mechanics* (Springer, New York, 1989).

[57] G. Adesso, A. Serafini, and F. Illuminati, *Extremal entanglement and mixedness in continuous variable systems*, *Phys. Rev. A* **70**, 022318 (2004).

[58] G. Vidal and R. F. Werner, *Computable measure of entanglement*, *Phys. Rev. A* **65**, 032314 (2002).

[59] G. Adesso and F. Illuminati, *Entanglement in continuous-variable systems: recent advances and current perspectives*, *J. Phys. A: Math. Theor.* **40**, 7821 (2007).

Supplemental Material for “Measurement-Induced Phase Transition in Free Bosons”

Kazuki Yokomizo¹ and Yuto Ashida^{1,2}

¹*Department of Physics, The University of Tokyo,
7-3-1 Hongo, Bunkyo-ku, Tokyo, 113-0033, Japan*

²*Institute for Physics of Intelligence, University of Tokyo, 7-3-1 Hongo, Tokyo 113-0033, Japan*

BOSONIC GAUSSIAN STATE AND ENTANGLEMENT ENTROPY

In this section, we define a bosonic Gaussian state and summarize its key results (see Ref. [1] for further details). We also explain how one can calculate the von Neumann entropy for a general bosonic Gaussian state, which measures the degree of quantum entanglement between a subsystem and the rest of the system. Suppose that N bosonic modes are described by a vector of the linear operators:

$$\hat{\phi} = (\hat{x}_1, \dots, \hat{x}_N, \hat{p}_1, \dots, \hat{p}_N)^T, \quad (\text{S1})$$

which satisfy the canonical commutation relations

$$[\hat{\phi}_j, \hat{\phi}_k] = i\sigma_{jk}, \quad \sigma = \begin{pmatrix} O & 1_N \\ -1_N & 0 \end{pmatrix}, \quad (\text{S2})$$

where 1_N is an $N \times N$ identity matrix, and we set $\hbar = 1$. Let $\hat{\rho}$ denote a density operator of an N -mode bosonic many-body state. The density operator can be represented as a quasiprobability distribution on the phase space in general. We define the displacement operator as

$$\hat{D}_{\xi} = \exp(i\hat{\phi}^T \sigma \xi), \quad (\text{S3})$$

where $\xi \in \mathbb{R}^{2N}$. The definition of the characteristic function then reads

$$\chi(\xi) = \text{Tr}(\hat{\rho} \hat{D}_{\xi}), \quad (\text{S4})$$

and the Wigner function is defined as

$$W(\zeta) = \int_{\mathbb{R}^{2N}} \frac{d^{2N}\xi}{(2\pi)^{2N}} \exp(-i\zeta^T \sigma \xi) \chi(\xi), \quad (\text{S5})$$

where $\zeta \in \mathbb{R}^{2N}$. We here remark that the statistical moments of $\hat{\phi}$ characterize the above phase-space representation. In particular, the defining features in the bosonic Gaussian state are the first moment defined as the mean value,

$$\phi = \langle \hat{\phi} \rangle = \text{Tr}(\hat{\rho} \hat{\phi}), \quad (\text{S6})$$

and the second moment defined as the covariance matrix,

$$(\Gamma_{\phi})_{jk} = \frac{1}{2} \langle \{ \delta\hat{\phi}_j, \delta\hat{\phi}_k \} \rangle \quad (\text{S7})$$

for $\mu, \nu = 1, \dots, 2N$, where $\delta\hat{\phi}_j = \hat{\phi}_j - \langle \hat{\phi}_j \rangle$. We note that the covariance matrix satisfies the Heisenberg uncertainty relation given by

$$\Gamma_{\phi} + \frac{i}{2}\sigma \geq 0, \quad (\text{S8})$$

where the equality holds when the quantum state is a pure state. A bosonic Gaussian state is fully characterized by the first and second moments. More specifically, the many-body state whose Wigner function can be written as the Gaussian form,

$$W(\zeta) = \frac{1}{(2\pi)^N \sqrt{\det \Gamma_{\phi}}} \exp \left[\frac{1}{2} (\zeta - \phi)^T \Gamma_{\phi}^{-1} (\zeta - \phi) \right], \quad (\text{S9})$$

are classified as the bosonic Gaussian state. One of the key properties of the Gaussian states is that any moments of $\hat{\phi}$ can be calculated from the first and second moments, which is nothing but Wick’s theorem. Let us consider the n -point correlation function defined by

$$C_n = \langle (\hat{\phi}_{j_1} - \phi_{j_1}) \cdots (\hat{\phi}_{j_n} - \phi_{j_n}) \rangle. \quad (\text{S10})$$

For a Gaussian state, any odd-ordered n -point correlation functions vanish, i.e.,

$$C_{2m+1} = 0, \quad (m \in \mathbb{N}), \quad (\text{S11})$$

while even-ordered n -point correlation functions can be represented by products of the two-point correlation functions [2].

We next derive the formula of the entanglement entropy for a bosonic Gaussian state. We consider the bipartition of the system into two subsystems A and \bar{A} , where A contains the N_A bosonic modes. Suppose that $\hat{\rho}_A = \text{Tr}_{\bar{A}} \hat{\rho}_G$ represents the reduced density operator of the subsystem A , where $\hat{\rho}_G$ is the density operator of the Gaussian state. We here focus on the von Neumann entropy between the subsystems A and \bar{A} , defined as

$$S_A = -\text{Tr}(\hat{\rho}_A \log \hat{\rho}_A). \quad (\text{S12})$$

It is worth noting that Eq. (S12) only depends on the covariance matrix $(\Gamma_{\phi})_A$ obtained from $\hat{\rho}_A$, since it is possible to arbitrarily adjust the first moment to be zero by local unitary operations. To calculate Eq. (S12), we recall Williamson’s theorem [3], which states that there exists a symplectic matrix \bar{S} diagonalizing the covariance matrix in the form of

$$\bar{S} (\Gamma_{\phi})_A \bar{S}^T = \text{diag}(\kappa_1, \dots, \kappa_{N_A}, \kappa_1, \dots, \kappa_{N_A}), \quad (\text{S13})$$

where κ_l ($l = 1, \dots, N_A$) are called symplectic eigenvalues. We note that all the symplectic eigenvalues take values greater than or equal to $1/2$ because of the Heisenberg uncertainty relation. Importantly, the matrix \hat{S} generates the unitary operator \hat{U} transforming $\hat{\rho}_A$ into the factorized form given by

$$\hat{\rho}_A = \hat{U} \hat{\rho}^{\otimes} \hat{U}^{\dagger}, \quad (\text{S14})$$

$$\hat{\rho}^{\otimes} = \bigotimes_{l=1}^{N_A} \hat{\rho}_l, \quad (\text{S15})$$

$$\hat{\rho}_l = \frac{1}{\kappa_l + 1/2} \sum_{n=0}^{\infty} \left(\frac{\kappa_l - 1/2}{\kappa_l + 1/2} \right)^n |n\rangle \langle n|, \quad (\text{S16})$$

where $|n\rangle$ is the n th Fock state [4]. Thus, the above representation allows us to calculate Eq. (S12) as follows:

$$\begin{aligned} S_A &= - \sum_{l=1}^{N_A} \text{Tr} (\hat{\rho}_l \log \hat{\rho}_l) \\ &= \sum_{l=1}^{N_A} \left[\left(\kappa_l + \frac{1}{2} \right) \log \left(\kappa_l + \frac{1}{2} \right) \right. \\ &\quad \left. - \left(\kappa_l - \frac{1}{2} \right) \log \left(\kappa_l - \frac{1}{2} \right) \right]. \end{aligned} \quad (\text{S17})$$

TIME-EVOLUTION EQUATION

In this section, we derive the time-evolution equation of the bosonic Gaussian state under continuous monitoring (see e.g., Ref. [5]). We consider an N mode bosonic Gaussian state $|\psi_G\rangle$. The dynamics of $|\psi_G\rangle$ under continuous monitoring can be described by the following stochastic Schrödinger equation:

$$\begin{aligned} d|\psi_G\rangle &= \left[-i\hat{H}dt - \frac{1}{2} \sum_n \left(\hat{\mathcal{O}}_n - \langle \hat{\mathcal{O}}_n \rangle \right)^2 dt \right. \\ &\quad \left. + \sum_n \left(\hat{\mathcal{O}}_n - \langle \hat{\mathcal{O}}_n \rangle \right) dW_n \right] |\psi_G\rangle, \end{aligned} \quad (\text{S18})$$

where \hat{H} and $\hat{\mathcal{O}}_n$ represent a Hamiltonian and measurement operators, respectively, dW_n is the Wiener increment which has the zero mean, $\mathbb{E}(dW_n) = 0$, and satisfies $dW_n dW_{n'} = \delta_{nn'} dt$, and $\langle \cdots \rangle = \langle \psi_G | \cdots | \psi_G \rangle$. We assume that the Hamiltonian can be written by the quadratic form,

$$\hat{H} = \sum_{j,k} h_{jk} \hat{\phi}_j \hat{\phi}_k, \quad (\text{S19})$$

with the symmetric matrix h and that the measurement operators are the linear combinations of $\hat{\phi}$,

$$\hat{\mathcal{O}}_n = \sum_j O_{nj} \hat{\phi}_j, \quad (\text{S20})$$

with the real-valued matrix O . In this case, the Gaussian state remains Gaussian during the whole stochastic time evolution. Thus, it is sufficient to consider only the time evolutions of the mean value

$$\phi = \langle \psi_G | \hat{\phi} | \psi_G \rangle \quad (\text{S21})$$

and the covariance matrix

$$(\Gamma_{\phi})_{jk} = \frac{1}{2} \langle \psi_G | \{ \delta \hat{\phi}_j, \delta \hat{\phi}_k \} | \psi_G \rangle \quad (\text{S22})$$

for $j, k = 1, \dots, 2N$, where $\delta \hat{\phi}_j = \hat{\phi}_j - \langle \hat{\phi}_j \rangle$. To derive the time-evolution equation of the first-moment of the Gaussian state, we note that, for an arbitrary operator \hat{M} , one can derive the following equation from Eq. (S18):

$$\begin{aligned} d\langle \hat{M} \rangle &= - \left(i \langle [\hat{M}, \hat{H}] \rangle + \frac{1}{2} \sum_n \langle [\hat{\mathcal{O}}_n, [\hat{\mathcal{O}}_n, \hat{M}]] \rangle \right) dt \\ &\quad + \sum_n \langle \{ \hat{\mathcal{O}}_n, \hat{M} \} - 2\langle \hat{\mathcal{O}}_n \rangle \hat{M} \rangle dW_n. \end{aligned} \quad (\text{S23})$$

Since we have the relations,

$$-i[\hat{\phi}_j, \hat{H}] = (\sigma h \hat{\phi})_j, \quad (\text{S24})$$

$$\langle [\hat{\mathcal{O}}_n, [\hat{\mathcal{O}}_n, \hat{\phi}_j]] \rangle = 0, \quad (\text{S25})$$

$$\langle \{ \hat{\mathcal{O}}_n, \hat{\phi}_j \} - 2\langle \hat{\mathcal{O}}_n \rangle \hat{\phi}_j \rangle = 2(\Gamma_{\phi} O^T)_{jn}, \quad (\text{S26})$$

Eq. (S23) allows us to derive the time-evolution equation of the mean value as follows:

$$d\phi = \sigma h \phi dt + 2\Gamma_{\phi} O^T dW, \quad (\text{S27})$$

where $dW = (dW_1, \dots, dW_N)^T$. To obtain the equation of motion for the second moment of the Gaussian state, we note that the derivative of the covariance matrix reads

$$\begin{aligned} d(\Gamma_{\phi})_{jk} &= \frac{1}{2} \left((d\langle \psi_G |) \{ \delta \hat{\phi}_j, \delta \hat{\phi}_k \} | \psi_G \rangle \right. \\ &\quad \left. + \langle \psi_G | \{ \delta \hat{\phi}_j, \delta \hat{\phi}_k \} (d|\psi_G\rangle) \right) - d\langle \hat{\phi}_j \rangle d\langle \hat{\phi}_k \rangle. \end{aligned} \quad (\text{S28})$$

where the last term is the correction term from the Itô formula. The first and second terms on the right-hand side of Eq. (S28) are represented by

$$\begin{aligned} &\frac{1}{2} \left((d\langle \psi_G |) \{ \delta \hat{\phi}_j, \delta \hat{\phi}_k \} | \psi_G \rangle + \langle \psi_G | \{ \delta \hat{\phi}_k, \delta \hat{\phi}_j \} (d|\psi_G\rangle) \right) \\ &= \frac{i}{2} \langle [\hat{H}, \delta \hat{\phi}_j \delta \hat{\phi}_k + \delta \hat{\phi}_k \delta \hat{\phi}_j] \rangle dt \\ &\quad - \frac{1}{4} \sum_n \langle [\hat{\mathcal{O}}_n, [\hat{\mathcal{O}}_n, \delta \hat{\phi}_j \delta \hat{\phi}_k + \delta \hat{\phi}_k \delta \hat{\phi}_j]] \rangle dt \\ &\quad + \frac{1}{2} \sum_n \langle \{ \hat{\mathcal{O}}_n, \delta \hat{\phi}_j \delta \hat{\phi}_k + \delta \hat{\phi}_k \delta \hat{\phi}_j \} \rangle \\ &\quad - 2\langle \hat{\mathcal{O}}_n \rangle (\delta \hat{\phi}_j \delta \hat{\phi}_k + \delta \hat{\phi}_k \delta \hat{\phi}_j) dW_n. \end{aligned} \quad (\text{S29})$$

All the terms on the right-hand side of Eq. (S29) are calculated as

$$\frac{i}{2} \left\langle [\hat{H}, \delta\hat{\phi}_j \delta\hat{\phi}_k + \delta\hat{\phi}_k \delta\hat{\phi}_j] \right\rangle = (\sigma h \Gamma_\phi)_{jk} + (\Gamma_\phi (\sigma h)^T)_{jk}, \quad (\text{S30})$$

$$-\frac{1}{4} \sum_n \left\langle [\hat{O}_n, [\hat{O}_n, \delta\hat{\phi}_j \delta\hat{\phi}_k + \delta\hat{\phi}_k \delta\hat{\phi}_j]] \right\rangle = (\sigma O^T O \sigma^T)_{jk}, \quad (\text{S31})$$

$$\left\langle \{\hat{O}_n, \delta\hat{\phi}_j \delta\hat{\phi}_k + \delta\hat{\phi}_k \delta\hat{\phi}_j\} - 2\langle \hat{O}_n \rangle (\delta\hat{\phi}_j \delta\hat{\phi}_k + \delta\hat{\phi}_k \delta\hat{\phi}_j) \right\rangle = 0, \quad (\text{S32})$$

where we use Eq. (S11) in Eq. (S32), and the last term on the right-hand side of Eq. (S28) is calculated as

$$d\langle \hat{\phi}_j \rangle d\langle \hat{\phi}_k \rangle = 4 (\Gamma_\phi O^T O \Gamma_\phi)_{jk}. \quad (\text{S33})$$

Therefore, we obtain the time-evolution equation of the covariance matrix as follows:

$$\frac{d\Gamma_\phi}{dt} = \sigma h \Gamma_\phi + \Gamma_\phi (\sigma h)^T + \sigma O^T O \sigma^T - 4 \Gamma_\phi O^T O \Gamma_\phi. \quad (\text{S34})$$

We here remark that Eq. (S34) is a deterministic equation in that it does not include stochastic terms, although the Gaussian state obeys the stochastic time evolution described by Eq. (S18). Physically, this means that the envelope of the Gaussian state behaves in the same manner during the evolution in any trajectory provided that the initial state is the same, while the center of the wave packet can fluctuate and exhibit the random motion influenced by continuous monitoring (cf. Eq. (S27)). In particular, we note that Eq. (S34) has a unique steady solution $d\Gamma_\phi/dt = 0$ in the limit of $t \rightarrow \infty$, independent of initial Gaussian states.

CORRELATION FUNCTION

In this section, we investigate the spatial correlation between the particles in the long-time limit under the local or nonlocal measurement. The strength of the correlation between \hat{x}_j and \hat{x}_k is given by the (j, k) element of the steady solution of Eq. (S34). We set $j = 1$ and the system size to be $L = 400$ in the following. Furthermore, let α_c denote the value of α at which the entanglement phase transition occurs. The entanglement entropy obeys the subvolume law at $\alpha < \alpha_c$, while it obeys the area law at $\alpha > \alpha_c$.

Figure S1 shows the scaling of the spatial correlation under the local or nonlocal measurement. In Fig. S1(a), the correlation almost does not decay in the case of $\alpha = 0.1, 0.3, 0.5$, while it exhibits the rapid decay in the case of $\alpha = 1.3, 1.5, 1.7$. The change of the behavior in the correlation occurs at $\alpha_c = 1$. Thereby, at $\alpha < \alpha_c$, the long-range correlation gives rise to the subvolume-law

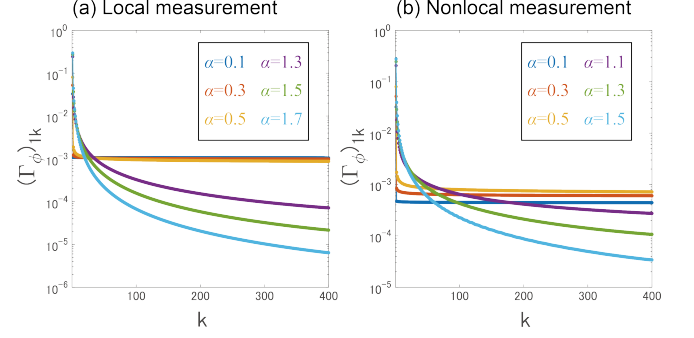


FIG. S1. (a,b) Spatial correlations under the (a) local or (b) nonlocal measurement. We show the $(1, k)$ elements of the covariance matrices in a semilogarithmic plot. We set the system size to be $L = 400$ and the measurement strength as $\gamma = 0.5$ in (a) and $\gamma = 0.01$ in (b).

phase, and at $\alpha > \alpha_c$, the rapidly decaying correlation leads to the area-law phase as we discuss in the main text.

Also, in Fig. S1(b), there exists the long-range correlation at $\alpha < \alpha_c$, while the rapidly decaying correlation appears at $\alpha > \alpha_c$. Meanwhile, we find that, at $\alpha < \alpha_c$, the correlation increases as α is increased, which is different from the behavior found in Fig. S1(a). This is consistent with our finding in the main text that the nonlocal measurement leads to the nonmonotonic behavior of the size-scaling exponent [Fig. 3(e) in the main text], where the bipartite entanglement is maximal around $\alpha \simeq 0.67$.

SCALING OF THE ENTANGLEMENT ENTROPY

In this section, we consider the setup with the short-range particle-particle coupling under the nonlocal measurement and show the scaling of the half-chain entanglement entropy. We focus on the entanglement entropy of the bosonic Gaussian state in the long-time limit similar to the above case. The considered setup obeys Eq. (S18) where the Hamiltonian is

$$\hat{H} = \sum_{j=1}^L \frac{\Omega}{2} (\hat{p}_j^2 + \hat{x}_j^2) + \sum_{j=1}^{L-1} \frac{K}{2} (\hat{x}_j - \hat{x}_{j+1})^2, \quad (\text{S35})$$

and the measurement operators are given by

$$\hat{O}_n = \sqrt{\frac{\gamma}{r^\alpha}} (\hat{x}_j \pm \hat{x}_{j+r}) \quad (\text{S36})$$

with $n = (j, r, \pm)$. For the sake of simplicity, we set $K = \Omega = 1$. Figure S2 shows the resulting entanglement scaling at different α . We find that, at any α , the entanglement entropy asymptotically converges a constant in the limit of $L \rightarrow \infty$ as indicated by black horizontal lines in Fig. S2. Thus, we conclude that the entanglement entropy in the setup always obeys the area law.

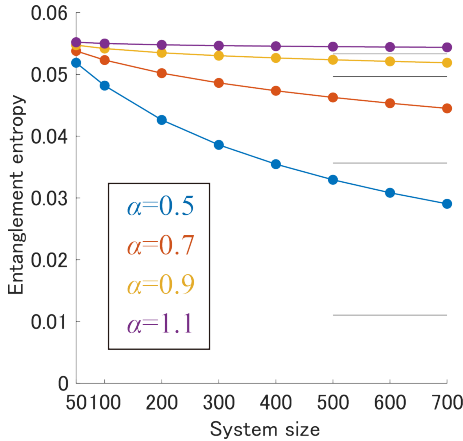


FIG. S2. Half-chain entanglement entropy in the setup where the coupling is short-ranged and the system is subject to the nonlocal measurement with $\gamma = 0.5$. We show the asymptotic values of the entanglement entropy by the black horizontal lines extracted from the fitting to $S = (A_0 + A_1 L) / (1 + B_1 L)$.

LOGARITHMIC NEGATIVITY

In this section, we calculate the logarithmic negativity of the bosonic (mixed) Gaussian state with the $N \in 2\mathbb{Z}$ bosonic modes, which is obtained by the ensemble average over the quantum trajectories. The half-chain logarithmic negativity is defined as

$$\mathcal{N}_A = \log \|\hat{\rho}^{T_A}\|_1, \quad (\text{S37})$$

where $\hat{\rho}^{T_A}$ represents the partial transpose of the original density matrix with respect to the half region A , and $\|\hat{\rho}^{T_A}\|_1$ represents the trace norm of $\hat{\rho}^{T_A}$ [6]. We remark that, for a bosonic Gaussian state, the logarithmic negativity only depends on the covariance matrix. Indeed, by defining

$$\mathcal{T}_A = 1_N \oplus (1_{N/2} \oplus (-1_{N/2})), \quad (\text{S38})$$

where 1_M is an $M \times M$ identity matrix, the partial transpose for the original covariance matrix Γ_ϕ is performed as

$$\tilde{\Gamma}_\phi = \mathcal{T}_A \Gamma_\phi \mathcal{T}_A. \quad (\text{S39})$$

Let $(\tilde{\kappa}_1, \dots, \tilde{\kappa}_N)$ denote the symplectic eigenvalues of the partially transposed covariance matrix. We then obtain the logarithmic negativity of the Gaussian state as follows [7]:

$$\mathcal{N}_A = \sum_{l=1}^N \log \max \left(1, \frac{1}{2\tilde{\kappa}_l} \right). \quad (\text{S40})$$

It is worth noting that, after taking the ensemble average over the quantum trajectories, the covariance matrix

obeys the time-evolution equation given by

$$\frac{d\Gamma_\phi}{dt} = \sigma h \Gamma_\phi + \Gamma_\phi (\sigma h)^T + \sigma O^T O \sigma^T. \quad (\text{S41})$$

One can thus track the time evolution of the logarithmic negativity. We show the numerical results under the local or nonlocal dissipation by using the above equations [Fig. S3], where $(\Gamma_\phi)_0 = (1/2) 1_{2N}$ is set as an initial state. We find that, in both cases, the logarithmic negativity vanishes in finite time.

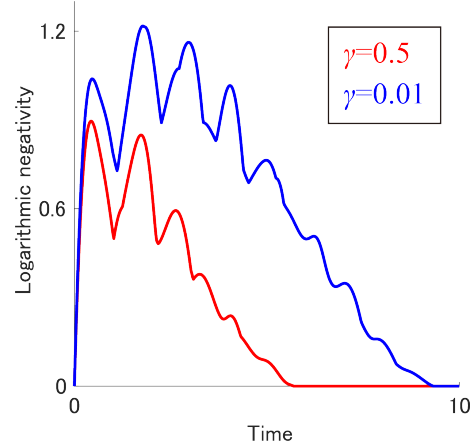


FIG. S3. Time evolutions of the half-chain logarithmic negativity under the local (red) or nonlocal (blue) dissipation. We set $L = 100$ and $\alpha = 0.7$ in both cases.

- [1] C. Weedbrook, S. Pirandola, R. García-Patrón, N. J. Cerf, T. C. Ralph, J. H. Shapiro, and S. Lloyd, *Gaussian quantum information*, *Rev. Mod. Phys.* **84**, 621–669 (2012).
- [2] L. Hackl and E. Bianchi, *Bosonic and fermionic Gaussian states from Kähler structures*, *SciPost Phys. Core* **4**, 025 (2021).
- [3] V. I. Arnold, *Mathematical Methods of Classical Mechanics* (Springer, New York, 1989).
- [4] G. Adesso, A. Serafini, and F. Illuminati, *Extremal entanglement and mixedness in continuous variable systems*, *Phys. Rev. A* **70**, 022318 (2004).
- [5] Y. Minoguchi, P. Rabl, and M. Büchholz, *Continuous gaussian measurements of the free boson CFT: A model for exactly solvable and detectable measurement-induced dynamics*, *SciPost Phys.* **12**, 009 (2022).
- [6] G. Vidal and R. F. Werner, *Computable measure of entanglement*, *Phys. Rev. A* **65**, 032314 (2002).
- [7] G. Adesso and F. Illuminati, *Entanglement in continuous-variable systems: recent advances and current perspectives*, *J. Phys. A: Math. Theor.* **40**, 7821 (2007).